

ARTICLE INFO

Received 13 November 2021

Accepted 20 November 2021

Available online December 2021

SYNTHESIS OF FLUORIDE NaYF₄/Yb/Tm, NaYF₄/Yb/Er MICRO- AND NANOCRYSTALS AND THEIR CHARACTERIZATION BY UV OPTICAL MICROSCOPY METHOD

V. I. Sokolov, I. M. Asharchuk, I. O. Goryachuk, S.I. Molchanova

*Federal Scientific Research Center "Crystallography and Photonics" RAS,
119333, Leninsky ave. 59, Moscow, Russia*

Abstract: Fluoride NaYF₄/Yb/Tm and NaYF₄/Yb/Er micro- and nanocrystals, which are in the cubic (alpha-) and hexagonal (beta-) phase, have been synthesized. The sizes, crystal structure and shape of crystals (phosphors) are characterized by methods of scanning electron microscopy and X-ray diffraction, as well as by high-resolution UV optical microscopy and confocal microscopy. The photoluminescence (PL) of individual phosphors and their agglomerates in upconversion was studied using IR laser pumping light with wavelength of 980 nm. It was shown that using UV microscopy with wavelength of 365 nm and confocal microscopy - with wavelength of 405 nm, it is possible to determine the size and shape of particles with diameter of 300 nm. These methods occupy an intermediate position between optical microscopy (within visible range) and electron microscopy in terms of spatial resolution and are useful while analyzing of nanophosphors with organic cladding based on oleic acid.

Keywords: fluoride micro- and nanocrystals, nanophosphors, rare-earth elements, photoluminescence, upconversion, UV optical microscopy, confocal microscopy.

Introduction

Fluoride NaYF₄/Yb/Tm and NaYF₄/Yb/Er micro- and nanocrystals (nanophosphors) doped with rare earth elements are widely used in various fields of science and technology (see reviews [1, 2]), for example, to create compact waveguide light amplifiers [3-5]. One of main methods for studying these objects is scanning- (SEM) and transmission (TEM) electron microscopy. Modern electron microscopes have an atomic resolution and make it possible to determine not only the size of nanoparticles, but also their crystal structure and elemental composition. At the same time, the disadvantages of electron microscopy include destructive effect of this method and low contrast while investigating of organic materials (for example, the organic cladding of nanophosphors),

which often requires deposition of thin metal films to object studied. In addition, the electron microscopy does not allow to study the photoluminescence of individual nanophosphors and their agglomerates in up- or downconversion. For this, one should use the methods of wide-field- [6] or near-field optical microscopy [7].

At the same time, the classical optical microscopy of visible (optical) range is not very suitable to analyze of micro- and nano-objects, since it does not provide the required spatial resolution. According to Rayleigh criterion, the resolution R of a wide-field optical microscope (i.e. minimum distance between two separate objects that can be resolved) is determined by following relationship [8]:

$$R = 0.61\lambda / NA \quad (1)$$

where λ is light wavelength, NA is numerical aperture of microscope objective. At the same time, for most microscopes operating within the optical wavelength range, even when using immersion objectives, the resolution is about 0.26 μm . As follows from formula (1), there are two possibilities for improving the resolution of optical microscope: first, to increase the numerical aperture NA of objectives, and secondly - to decrease the wavelength λ of illuminating radiation. At present, the practical limit of increasing the numerical aperture of objectives has been reached. "Dry" objectives with NA = 0.95 and immersion objectives with NA = 1.45 have been created and presented at the market of scientific instruments. In 2020, Olympus Co. announced the creation of world's first immersion objective with numerical aperture of 1.50 [9]. The creation of immersion objectives with a significantly larger numerical aperture is apparently impossible due to fundamental physical limitations determined by properties of known optical materials. Thus, a further increase in resolution of optical microscopy can be achieved only by decreasing of wavelength λ , i.e. by going to UV band.

From the beginning of 21st century there has been significant progress in the development of optical microscopes that operate in UV spectrum band and have significantly better resolution than microscopes in the optical band. This progress is associated, on the one hand, with the needs of microelectronics (related with reduction of electronic elements on silicon chip in size, with development of high-precision masks for UV photolithography, etc.), and, on the other hand, with emergence of new high-precision technologies for creating optical objectives for microscopes. Currently, the world's leading microscope manufacturers are conducting research in the field of deep UV optical microscopy, which provides ultra-high lateral resolution. For example, Leica Microsystems Co. (Germany) presented the research microscope DM12000_M at the scientific instrument market, which allows research at a wavelength of 365 nm and provides the resolution of

$R \gg 140$ nm [10]. In addition, this company has developed the research microscope operating near wavelength of 248 nm [11-13]. This microscope is equipped with 150x "dry" objective with NA = 0.90, and 200x "immersion" objective with NA = 1.20. These objectives that created by Leica Co., are achromatic in 248 ± 8 nm wavelength range and provide the resolution of 100 and 80 nm, respectively. In 2005, Olympus Co. (Japan) introduced at the scientific instruments market U-UVF248 the attachment for optical microscopes, which allows one to study nanoscale objects at a wavelength of 248 nm [14] with resolution of 80 nm. Research investigation is carried out to create optical microscopes for even shorter wavelengths, in particular, at $\lambda = 193$ nm [15]. Table 1 gives an overview of limiting resolution R for optical microscope that can be achieved using "dry" and immersion objectives with different numerical apertures for different operating wavelengths [11].

Table 1. Resolution R of optical microscope depending on the light wavelength λ (WI - water immersion, OI - oil immersion).

Light wavelength λ , nm	405	365	365 (OI)	248	248 (WI)	193	193 (WI)
Numerical aperture	0.95	0.95	1.30	0.90	1.25	0.90	1.30
Resolution R , nm	260	234	171	168	121	130	90

This paper reports about synthesis of fluoride micro- and nanocrystals NaYF₄/Yb/Tm, NaYF₄/Yb/Er, coated with organic cladding based on oleic acid, and their characterization using wide-field UV optical microscopy and confocal microscopy.

Synthesis of fluoride micro- and nanocrystals

To obtain fluoride NaYF₄/Yb/Tm, NaYF₄/Yb/Er micro- and nanocrystals (phosphorus), the commercial reagents were used: oxides of yttrium, ytterbium, thulium, erbium, sodium carbonate, oleic acid 90%, 1-octadecene 90% (Sigma-Aldrich) and trifluoroacetic acid 99% (PanReac). Sodium oxides and carbonate were used without pretreatment. Trifluoroacetic acid was purified by distillation and diluted with distilled water to 50% vol. Synthesis of phosphorus was carried out by thermal decomposition of trifluoroacetates of rare earth elements Y, Yb, Tm, Er, obtained from corresponding oxides, as well as sodium trifluoroacetate, obtained from its carbonate. This reaction was carried out in oxygen-free medium in oleic acid/1-octadecene mixture by heating in the bath with Rose's alloy to 260-320°C [16-18]. Details of this method are presented in [18].

The growth of crystal sizes in the course of thermal synthesis was monitored by the change in integrated intensity $I_{\text{int_PL}}$ and by photoluminescence (PL) spectrum of reaction mixture in upconversion within a spectral range of 400-900 nm. The photoluminescence of nanoparticles in

solution was excited using special fiber-optic and diode laser radiation at a wavelength of 980 nm. The probe contained a pumping silica fiber and also - a receiving fiber, which captured the PL signal from nanoparticles in the flask and directed it to FSD-10 mini-spectrometer (R@DC Fiber Optic Devices, Russia). To cut off the pump radiation, we used SZS25 colored glass filters. In Fig. 1a shows the dependences of $I_{\text{int_PL}}$ on the synthesis time t of NaYF₄/Yb/Tm crystals, and Fig. 1b shows its I_{PL} PL spectra obtained at different time intervals after heating was switched on. The PL peaks in upconversion at a wavelengths of 474, 650 and 800 nm are due to energy structure of rare earth Tm³⁺ ions in NaYF₄/Yb/Tm crystal, specifically, by transitions $^1G_4 \rightarrow ^3H_6$, $^1G_4 \rightarrow ^3F_4$ и $^3H_4 \rightarrow ^3H_6$ [2].

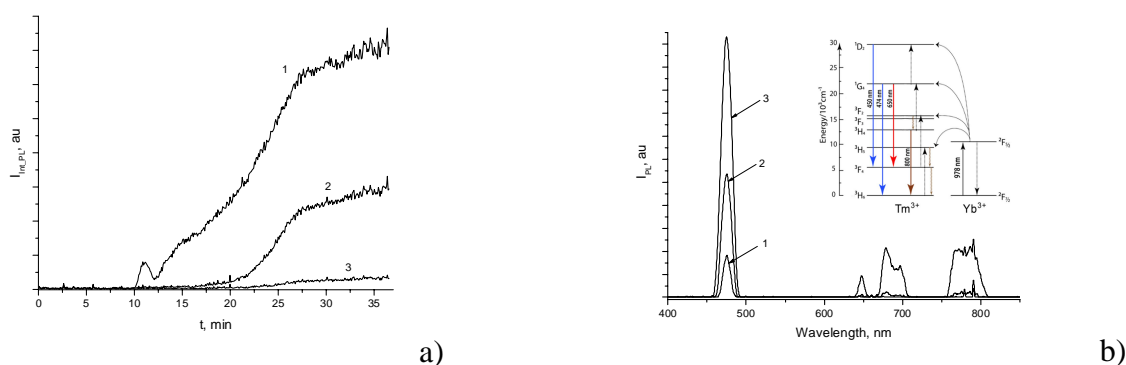


Figure 1. (a) Time dependences of integral intensity I_{PL} PL of *a*-NaYF₄/Yb/Tm phosphors at a wavelength ranges of 480 ± 25 nm, 650 ± 20 nm and 790 ± 45 nm. (b) I_{PL} PL spectrum for IPL nanoparticles after 13 (1), 21 (2), 37 min (3) after heating on. The inset shows a simplified system of Yb and Tm energy levels. Arrows indicate the radiative transitions.

As seen from Fig. 1a, PL intensity of NaYF₄/Yb/Tm particles in upconversion begins to increase sharply after the end of induction period, which at a synthesis temperature of 290°C lasts about 10 min from the moment of heating switches from 93 to 290°C. By the 27th min, the growth of PL decreases and subsequently it changes slightly. As a result of synthesis in oleic acid/1-octadecene solution, *a*-NaYF₄/Yb/Tm particles were formed. In Fig. 2 shows the SEM photograph and X-ray diffraction pattern of synthesized particles. The particles shown in Fig. 2a, are in the cubic *a*-phase. This is confirmed by diffraction pattern (see Fig. 2b), the peaks of which correspond to pure *a*-phase of NaYF₄/Yb/Tm crystals. As follows from Fig. 2a, diameter of particles is 10-20 nm.

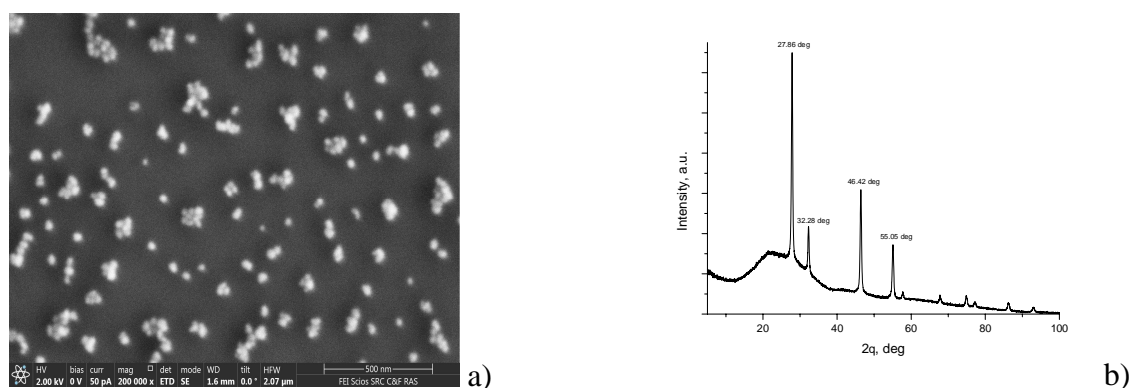


Figure 2. Photograph of synthesized α -NaYF₄/Yb/Tm nanoparticles obtained via scanning electron microscope (a), and their diffractogram obtained via Rigaku Miniflex600 X-ray diffractometer (Cu, $\lambda = 1.54184 \text{ \AA}$) (b). θ is angle of incidence of X-ray beam on the sample.

From Fig. 1a it can be seen that formation of α -NaYF₄/Yb/Tm particles is accompanied by increase in their photoluminescence. This makes it possible to control the size of synthesized phosphorus, and stopping the reaction at different points in time, at which PL intensity reaches a certain level. The synthesis reaction is stopped by quickly removing the flask with reaction solution from the bath with Rose's alloy and adding to the flask the cooled 1-octadecene, which leads to a sharp temperature decrease of solution by 100-120°C. In Fig. 3 shows size distribution histograms of α -NaYF₄/Yb/Tm nanoparticles obtained when this reaction was stopped at different times after start of reaction mixture heating. The nanoparticle sizes were measured by dynamic light scattering in chloroform via Brookhaven 90Plus_Zeta particle/protein analyzer (Brookhaven Instruments Co., USA) under illumination by laser at a wavelength of 640 nm. Note that dynamic light scattering method determines not the "true" size of nanoparticles, but their hydrodynamic diameter. In addition, the synthesized phosphorus is covered, as a rule, with organic cladding (see Fig. 4). Therefore, presented below results is the "upper-bound estimate" for diameter D of these nanoparticles.

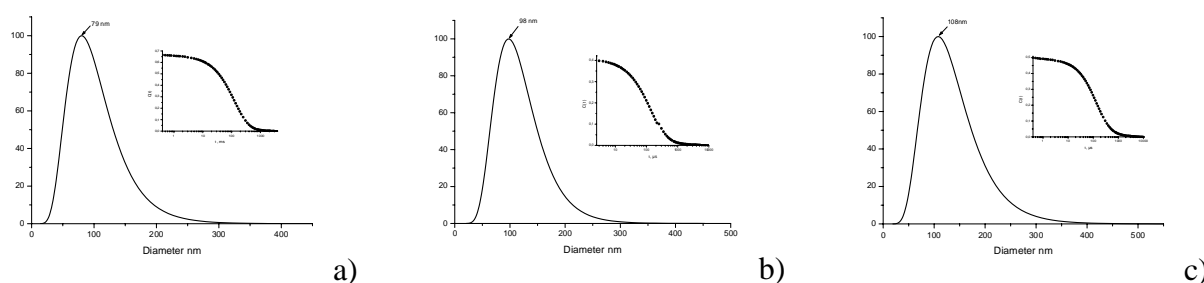


Figure 3. Histograms of nanoparticles size distribution of α -NaYF₄/Yb/Tm nanoparticles measured via Brookhaven 90Plus_Zeta particle/protein analyzer. D is hydrodynamic diameter of nanoparticles. Synthesis process was stopped after 12 min (a), 16 min (b), and 28 min (c). The insets show the corresponding autocorrelation functions.

As follows from Fig. 3, the average size (hydrodynamic diameter) of NaYF₄/Yb/Tm nanocrystals in organic cladding is 79 nm, 98 nm and 108 nm when reaction process is stopped after 12, 16 and 28 min, respectively.

In Fig. 4 shows the dependence of average particle diameter D on synthesis time. It follows from the comparison Fig. 4 and Fig. 1 that there is a clear correlation between the size of synthesized nanophosphors and photoluminescence intensity of reaction mixture. This fact is important because it allows you to stop the reaction at the time when the particle size reaches the target value.

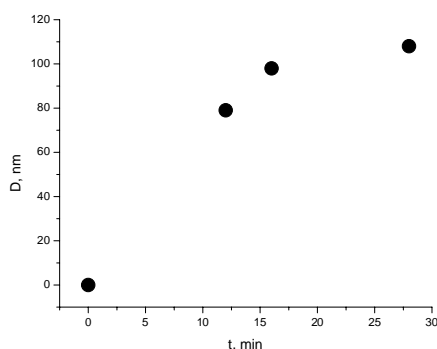


Figure 4. Average size (hydrodynamic diameter) D of α -NaYF₄/Yb/Tm nanoparticles coated with organic cladding, depending on duration of synthesis. t is the time from start of reaction mixture heating to termination of this reaction

As noted above, the synthesis of fluoride micro- and nanocrystals NaYF₄/Yb/Tm, NaYF₄/Yb/Er was carried out in oleic acid/1-octadecene mixture. This leads to the fact that the particles obtained during this synthesis are, as a rule, in organic cladding based on oleic acid [16-18]. In Fig. 5 shows the transmission spectrum of α -NaYF₄/Yb/Tm nanophosphorus powder at KBr substrate. The absorption band near 3464 cm⁻¹ can be associated with O-H compression vibrations. Strong absorption peaks near 2853 and 2924 cm⁻¹ are associated with symmetric and asymmetric vibrations of C-H of organic cladding of oleic acid nanoparticles. Additionally, the peaks near 1556 and 1463 cm⁻¹ are apparently due to asymmetric and symmetric vibrations of carboxyl COO groups, respectively [3]. Thus, from the analysis of Fig. 5, it can be concluded that all nanoparticles are coated with organic cladding based on oleic acid.

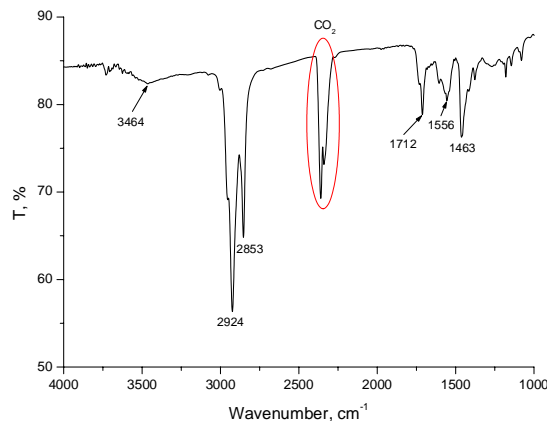


Figure 5. Transmission spectrum of *a*-NaYF₄/Yb/Tm nanoparticles at KBr substrate. The absorption bands and lines are due to organic oleic acid cladding of particles.

Study of micro- and nanocrystals *b*-NaYF₄/Yb/Er using wide-field UV microscopy

For analysis of phosphors with a size of 300-1500 nm, coated with organic cladding based on oleic acid, application of UV optical microscopy method has a number of advantages over electron microscopy. This is due to the fact that organic cladding of particles has a small contrast and is poorly visible when electron beam irradiated. At the same time, the cladding contrast strongly depends on wavelength of optical radiation, which makes it possible to study in detail both the particle itself (for example, when using immersion objectives and light radiation within a range of 340-750 nm), and its cladding, using "dry" objectives and light radiation with shorter wavelengths for which the organic cladding is poorly transparent.

Study of microparticles was carried out via Neophot-32 optical microscope (Zeiss Co., Germany), modernized to operate within a UV wavelength range from 340 nm. This microscope was equipped with SCM2020-UV CCD camera (EHD imaging GmbH, Germany) with 2048' 2048 pixels, 6.5' 6.5 μm each, and sensitive within a range 200-1100 nm. The object under study was illuminated by DRSh250-2 mercury lamp according to Koehler method. A research sample was prepared as follows: a drop of hexane with phosphorus particles dissolved in it was placed at the silicon substrate and heated at 100°C for 60 min until the solvent completely evaporated. In Fig. 6 shows photographs of *b*-NaYF₄/Yb/Er particles.

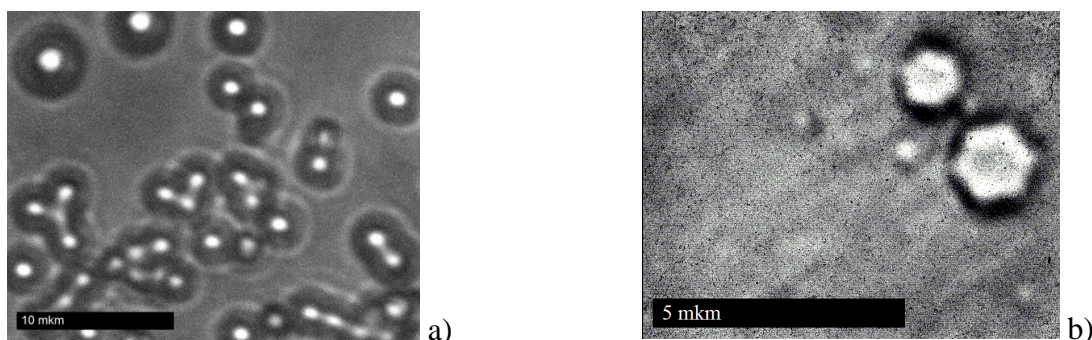


Figure 6. Photographs of *b*-NaYF₄/Yb/Er particles at the silicon substrate, obtained via Neophot-32 optical microscope. (a) $l = 355$ nm, “dry” objective 50x/0.90. The organic cladding of these particles is visible. (b) $l = 405$ nm, immersion objective 100x/1.30. Diameter of large hexagonal particle is $1.5 \mu\text{m}$, and diameter of small hexagon is $1.1 \mu\text{m}$. Visible particle diameter to left of this hexagon is $0.3 \mu\text{m}$.

As follows from Fig. 6a, diameter of organic particles claddings can be 4 or more times the diameter of particle itself, which leads to a difference in measured particle sizes using scanning electron microscopy and dynamic light scattering methods. In Fig. 6b, the hexagonal shape of two particles with diameters $d \gg 1.5$ and $1.1 \mu\text{m}$ is clearly visible, which indicates that these particles are in hexagonal *b*-phase. From Fig. 6b it also follows that, as a synthesis result, in addition to particles within the order of 1 micron, the smaller particles with a diameter of $\gg 300$ nm are formed (upper-bound estimate). The shape of these particles is not determined due to limited resolution of Neophot-32 microscope at a wavelength of 355 nm. Using of optical microscope with immersion objectives, larger numerical aperture (for example, $NA = 1.5$) and shorter wavelength $l = 248$ nm will allow to analysis of nanophosphors with a diameter from $\gg 200$ nm.

Study of size and shape of phosphors by confocal laser microscopy

Analysis of phosphors size coated with organic cladding based on oleic acid was also carried out via LEXT OLS3100 confocal scanning laser microscope (Olympus Co., Japan) at a wavelength of 405 nm. It is known that resolution R of confocal microscope is determined by following relationship:

$$R \gg 0.44 l / NA \quad (2)$$

Comparison of formulas (2) and (1) shows that resolution of confocal microscope is approximately 1.39 times better than the resolution of wide-field optical microscope with the same wavelength. This is due to the fact that diameter of Airy disk in confocal microscope is somewhat smaller than in wide-field microscope. In Fig. 7 shows photographs of *b*-NaYF₄/Yb/Er nanoparticles at silicon substrate, obtained via LEXT OLS3100 confocal microscope with

100x/0.80 "dry" objective and a 100x/1.00 water-immersed objective. One can see both individual particles with diameter of $d \gg 300$ nm in organic cladding and agglomerates of particles.

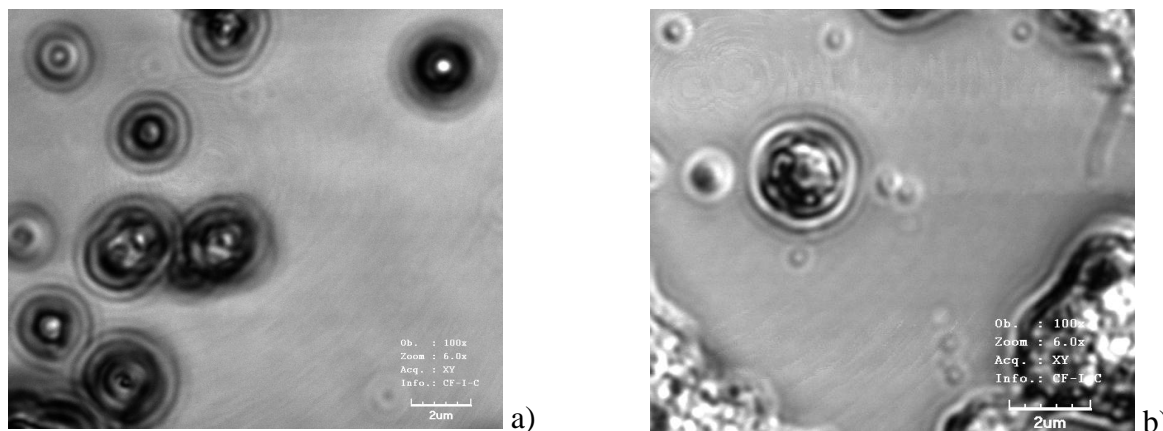


Figure 7. Photographs of *b*-NaYF₄/Yb/Er phosphors at silicon substrate, obtained via LEXT OLS3100 confocal laser microscope ($\lambda = 405$ nm). (a) "Dry" objective 100x/0.80. Individual particles with diameter of $d \gg 300$ nm in organic cladding are visible. (b) Immersion objective 100x/1.00. Both individual nanoparticles and their agglomerates are observed.

Study of photoluminescence of micro- and nanocrystals and their agglomerates

Micro- and nanocrystals NaYF₄/Yb/Er, NaYF₄/Yb/Tm have a complex photoluminescence spectrum in upconversion. In Fig. 8 shows photographs of luminescent *b*-NaYF₄/Yb/Er microparticles and their agglomerates in optical spectral range, obtained via Neophot-32 optical microscope with 50x/0.90 "dry" objective. The pumping system included a semiconductor laser emitting at a wavelength of 980 nm, equipped with fiber-optic cable with collimator and 20x objective (see inset to Fig. 8).

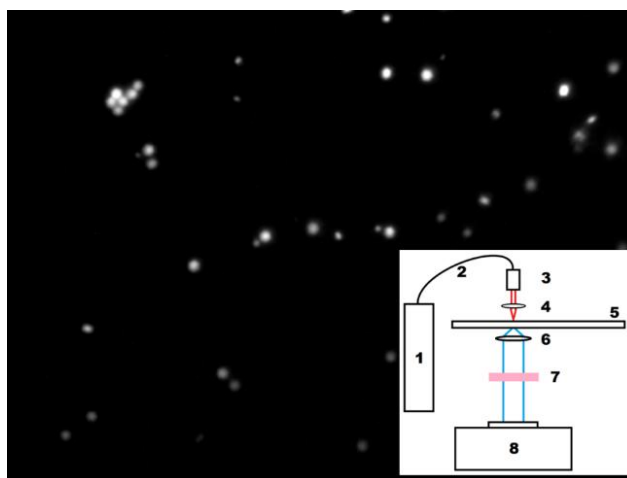


Figure 8. Photograph of luminescent *b*-NaYF₄/Yb/Er particles pumped by IR light radiation at a wavelength of 980 nm. The inset here shows the installation diagram for studying the PL spectra of particles and their agglomerates in upconversion. 1 - pumping laser, 2 - fiber-optic cable, 3 -

collimator, 4 - 20x objective, 5 - stage for sample, 6 - Neophot-32 microscope objective, 7 - optical filter that cuts off pumping radiation, 8 - CCD camera

Results and discussion

The authors studied the synthesis of micro- and nanocrystals $\text{NaYF}_4/\text{Yb}/\text{Tm}$, $\text{NaYF}_4/\text{Yb}/\text{Er}$ with cubic- (alpha) and hexagonal (beta) phases (micro- and nanophosphors) by thermal decomposition of trifluoroacetates of rare earth elements and sodium in oxygen-free medium and oleic acid/1-octadecene solution.

Process of phosphorus formation was monitored by measuring the intensity and photoluminescence spectrum of reaction mixture in upconversion when pumped by laser radiation at a wavelength of 980 nm. It was shown that photoluminescence of initial mixture is absent and begins to increase after the end of induction period, which is associated with nucleation and growth of phosphors. A clear correlation was established between the size of nanocrystals and PL intensity of this mixture. This makes it possible to stop the reaction at the moment when particle size reaches the target value. The size, crystal structure and shape of synthesized phosphors have been characterized by high-resolution UV optical microscopy and confocal microscopy. It is shown that using wide-field microscopy at a wavelength of 355 nm and confocal microscopy at a wavelength of 405 nm, it is possible to determine the size and shape of particles with a diameter of 300 nm. These methods occupy an intermediate position between optical microscopy of optical range and electron microscopy in terms of spatial resolution, and are useful while analyzing of nanophosphors with organic cladding based on oleic acid.

The synthesized nanophosphors can be used to create various active integrated optics devices, in particular, upconversion waveguide lasers and waveguide amplifiers for telecommunication C - wavelength range of 1530-1565 nm.

Conclusion

The authors have synthesized the fluoride crystalline micro- and nanoparticles $\text{NaYF}_4/\text{Yb}/\text{Tm}$, $\text{NaYF}_4/\text{Yb}/\text{Er}$, which are in cubic- (alpha) and hexagonal (beta) phases. The crystal growth process was monitored by the change in their PL spectra in upconversion directly during the synthesis. The resulting particles are coated with organic cladding based on oleic acid. It was shown that using wide-field UV optical microscopy and confocal microscopy, it is possible to determine the size and shape of nanoparticles within a range from 300 nm. We believe that using of confocal optical microscope with objectives with a larger numerical aperture (for example, with $\text{NA} = 1.5$) and transition to a shorter wavelength of 248 nm will make it possible to analyze nanocrystals with a diameter of 200 nm or less.

Acknowledgments

This work was financially supported by the Ministry of Science and Higher Education of the Russian Federation within the State assignment FSRC «Crystallography and Photonics» RAS in part of the study of the photoluminescent properties of fluoride nanocrystals doped with rare earth elements and the Russian Foundation for Basic Research (grant no. 20-07-01038) in part of the synthesis of nanophosphors. The authors are grateful to G.V. Mishakov, D.N. Karimov, V.V. Grebenev for their help in carrying out the experiments. The equipment of the Center for Collective Use of the Federal Research Center "Crystallography and Photonics" of the Russian Academy of Sciences was used.

References

1. H.A. Hoeppe, Recent developments in the field of inorganic phosphors, *Angew. Chem., Int. Ed.*, **2009**, 48, 3572-3582.
2. D.N. Karimov, P.A. Demina, A.V. Koshelev, V.V. Rocheva, A.V. Sokovikov, A.N. Generalova, V.P. Zubov, E.V. Khaydukov, M.V. Koval'chuk, V.Y. Panchenko, Upconversion nanoparticles: synthesis, photoluminescence properties, and applications, *Nanotechnologies in Russia*, **2020**, 15(6), 699-724. (in Russian)
3. X. Zhai, J. Li, Sh. Liu, X. Liu, D. Zhao, F. Wang, D. Zhang, G. Qin, W. Qin, Enhancement of 1.53 μm emission band in $\text{NaYF}_4:\text{Er}^{3+}, \text{Yb}^{3+}, \text{Ce}^{3+}$ nanocrystals for polymer-based optical waveguide amplifiers, *Optical Materials Express*, **2013**, 3(2), 270-277.
4. Y. Wang, X. Guo, Sh. Liu, K. Zheng, G. Qin, W. Qin., Controllable synthesis of $\beta\text{-NaLuF}_4:\text{Yb}^{3+}, \text{Er}^{3+}$ nanocrystals and their application in polymer-based optical waveguide amplifiers, *Journal of Fluorine Chemistry*, **2015**, 175, 125-128.
5. V.I. Sokolov, I.M. Asharchuk, S.I. Molchanova, M.M. Nazarov, A.V. Nechaev, K.V. Khaydukov, Optical amplifier for C-band based on polymer waveguide with embedded nanophosphors doped with rare earth elements, *Materials of the IV International Scientific Conference "Problems of Interaction of Radiation with Matter"*, Gomel, **2016**, 2, 127-132. (in Russian)
6. Q. Zhan, H. Liu, B. Wang, Q. Wu, R. Pu, C. Zhou, B. Huang, X. Peng, H. Agren, S. He, Achieving high-efficiency emission depletion nanoscopy by employing cross relaxation in upconversion nanoparticles, *Nat. Commun.*, **2017**, 8, 1058.
7. P. Bazylewski, S. Ezugwu, G. Fanchini, A Review of Three-Dimensional Scanning Near-Field Optical Microscopy (3D-SNOM) and Its Applications in Nanoscale Light Management, *Appl. Sci.*, **2017**, 7, 973.

8. G.S. Landsberg, Optics, Moscow, "Nauka", **1976**, 928 p. (in Russian)
9. <https://www.olympus-global.com/news/2019/nr01286.html>.
10. <https://www.leica-microsystems.com/products/light-microscopes/p/leica-dm12000-m/>.
11. W. Vollrath, Ultra-high-resolution DUV Microscope Optics for Semiconductor Applications, Proc. of SPIE, **2005**, 5865, 58650E.
12. T. Sure, T. Bauer, J. Heil, J. Wesner, DUV-Microscope objectives: technology driver that forces the production to switch from the micrometer scale to the nanometer scale, Proc. of SPIE, **2005**, 5965, 59651H.
13. U. Huebner, W. Morgenroth, R. Boucher, M. Meyer, W. Mirande, E. Buhr, G. Ehret, G. Dai, T. Dziomba, R. Hild, T. Fries, A nanoscale linewidth/pitch standard for high-resolution optical microscopy and other microscopic techniques, Measurement Science and Technology, **2007**, 18(2), 422-429.
14. https://www.olympus-ims.com/ru/microscope/u_uvfv248/.
15. G. Ehret, F. Pilarski, D. Bergmann, B. Bodermann, E. Buhr, A new high-aperture 193 nm microscope for the traceable dimensional characterization of micro- and nanostructures, Measurement Science and Technology, **2009**, 20(8), 1-10.
16. Mai H.-X., Zhang Y.-W., Si R., Yan Z.-G., Sun L.-D., You L.-P., Yan Ch.-H, High-Quality Sodium Rare-Earth Fluoride Nanocrystals, Controlled Synthesis and Optical Properties, J. Am. Chem. Soc., **2006**, 128(19), 6426-6436.
17. S. Alyatkin, I. Asharchuk, K. Khaydukov, A. Nechaev, O. Lebedev, Y. Vainer, V. Semchishen, E. Khaydukov, The influence of energy migration on luminescence kinetics parameters in upconversion nanoparticles, Nanotechnology, **2017**, 28, 035401.
18. V.I. Sokolov, I.M. Asharchuk, E.N. Glazunova, I.O. Goryachuk, A.V. Lyubeshkin, Synthesis of β -NaYF₄/Yb⁺³/Er⁺³ fluoride nanocrystals at high pressure, Fluorine Notes, **2021**. 1(134), 1-2.